BULLETIN OF THE POLISH ACADEMY OF SCIENCES
TECHNICAL SCIENCES, Vol. 68, No. 1, 2020
DOI: 10.24425/bpasts.2020.131830

Optimization of process parameters of friction stir welded AA5082-AA7075 butt joints using resonance fatigue properties

G. KUMAR, R. KUMAR and R. KUMAR*

Mechanical Engineering Department, Birla Institute of Technology, Mesra, Ranchi, 35215, Jharkhand, India

Abstract. In this work, experiments were carried out to quantify the behaviour of friction stir welded (FSW) AA5082-AA7075 butt joints under tensile loading and completely reversed fatigue loading. Different samples were prepared to identify optimum tool rotational and travel speeds to produce FSW AA5082-AA7075 butt joints with the maximum fatigue life. ANOVA was performed, which confirmed that both tool speed and tool rotational speed affect the tensile strength of the weld. The samples exhibit a considerable difference in their fatigue life and tensile strength. This difference can be accounted to the presence of welding defects such as surface defects and porosity. S-N curve plotted for the sample shows a significantly high fatigue life at the lower stress ranges. Fracture surfaces were also analysed under scanning electron microscope (SEM). Study of the fracture surface of the sample that failed under fatigue loading showed that the surface was mainly divided in two zones. The first zone was the area of fatigue crack growth where each stress cycle, slowly and gradually, helped in the growth of the crack. The second zone was the region of fast fracture where the crack growth resulted in the failure of the joint instantaneously. The fracture surface study of the sample that failed under tensile loading showed that the mode of failure was ductile in nature.

Key words: friction Stir Welding, Dissimilar Al Welding, Resonance Fatigue Analysis, Fracture Surface Analysis, ANOVA.

1. Introduction

The demand for alloys with high strength to weight ratio is increasing in recent times. These alloys have high demand in industries like automotive, aerospace, aeronautics, railways and naval industries. In this scenario, aluminium alloys are a good option due to their high strength to weight ratio and having better resistance to corrosion. Al-alloys are difficult to-weld by conventional fusion joining techniques [7, 9, 10, 41] in which several problems such as porosity formation and cracking are encountered. To avoid or minimize these problems the heat input should be kept as low as possible during joining process. One way of doing this is the use of FSW in which the heat input is low since it is a solid state joining technique [2, 4, 5, 8, 27]. In order to survive in this competitive world, these industries are consistently finding for methods to reduce costs while maintaining the high standards for materials and processes. Nowadays, industries are using friction stir welding (FSW) process to weld these alloys [38]. A few companies have already started using FSW for the manufacturing of their products and services for its cost saving advantages [39]. Although the welding of dissimilar metals or metal matrix composites is a very new process, recent studies have been made for dissimilar welding of aluminium alloys using FSW.

Frictional heat has been used as a solid-phase welding technique for over a century. However, there was no technological advancement in the field of friction welding [49]. The researchers at the Welding Institute invented and patented a new solid-phase welding technique known as the FSW [48]. In FSW, the welding occurs at a temperature lower than the melting point of the material, this helps the material to retain its parent mechanical properties. Also, the FSW joint displays better strength properties than TIG and MIG welded joints [26]. This is because all the problems associated to the solidification of the welded region are avoided as the welding occurs in visco-plastic solid phase. It produces welds that have good quality. It is difficult or even impossible to weld dissimilar metallic materials using fusion methods. Fusion methods result in cracking, voids, distortion and/or the heat affected zone (HAZ) which becomes excessively soft. FSW has the benefit of being able to weld dissimilar metallic materials without the introduction of these defects. It is also a clean and ecological technique [46,47].

2. State of art

Dubourg et al. optimized the friction stir lap welds process for different alloys. In their experiment best fatigue life was found for the double pass welded samples keeping overlapping in advancing side [14]. Ericsson et al. investigated the influence of process parameter on fatigue life of FSW samples. They observed that at very low welding speed, fatigue life was increased due to increased amount of heat input per unit length of weld [17]. Lee et al. studied the lap joint properties of dissimilar FSW joints. They concluded that interface morphology was the main factor for predicting the strength of FSW lap joints [36]. Miller et al. investigated the development

*e-mail: ratan_876@yahoo.co.in

Manuscript submitted 2019-10-22, revised 2019-12-11, initially accepted for publication 2019-12-12, published in February 2020

in automotive industry for the use of aluminium alloys. They suggest to improve the aluminium scrap recycling by introducing unialloy system [37]. Nandan et al. studied the recent advances in the field of friction stir welding process. Their review gives the understanding of process and its metallurgical aspects [40]. Rao et al. made a comprehensive study on fatigue and fracture properties of dissimilar FSW joint to aluminium with magnesium alloys. Through fractographic analysis they concluded that fatigue cracks initiated at weld cracks area [43]. Rodriguez et al. conducted an experimental analysis for low cycle fatigue behaviour of dissimilar FSW joints of aluminium alloys. They studied the fracture surface using scanning electron microscope. By their study they concluded that crack initiated at either the crown or at the root of the welded joints [44]. Feng et al. studied the effect of varying tool feed and rotational speed on the microstructural and fatigue behaviour of FSWed AA7075 alloy. They observed two low hardness zones between TMAZ and HAZ and the failure of the samples with lower welding feed occurred in these low hardness zones. Also, samples prepared at higher welding feed failed in the nugget zone [18]. Infante et al. studied the fatigue behaviour of the dissimilar FSWed AA6082 and AA5754 alloys. Their results exhibited that for the lower applied stress ranges, fatigue life of the FSWed AA6082 and AA5754 joints had a better fatigue performance [20]. Çam et al. established that there is a loss in the strength in the welded region, inspite of the the sound weld quality. They also exhibitted that during FSW, the strength of the nugget could be enhanced by using high strength interlayer. However, the external cooler used was not sufficient to achieve the adequate cooling conditions for improved strength [6].

Cavaliere et al. studied the effect of process parameters on the properties of dissimilar friction stir welded joints. They also conducted the fatigue test at the axial total stress amplitude control mode. They concluded that the main reason for the fatigue fracture is the presence of forging defects in joints [11]. Crawford et al. studied the defect development in the AA6061-T6 FSWed joints, prepared at varying tool feed and rotational speed. They observed two types of defects, wormholes and weld deformations, owing to these varying parameters [13]. İpekoğlu and Çam produced dissimilar AA7075-O/6061-O and AA7075-T6/6061-T6 butt joints using FSW and postwelding heat treatments were performed on the joints obtained. They observed that hardness increase was obtained for O-temper produced joints wheras hardness loss was obtained for T6 temper produced joints. They also obseved that the postwelding heat treatment improved the joint properties [21]. Bozkurt et al. investigated the effect of plate positioning, plunge depth, dwell time and tool tilt angle on dissimilar friction stir spot welded AA 5754-H22/2024-T3 joints. They observed that plate positioning was crucial for the joint strength. Higher joint strenght was obtained when AA5754 was on top in comparison to when AA2024 was placed on top. Plunge depth, dwell time and tool tilt angle affected the failure mode of the friction stir spot welded lap joints produced [1]. Kim et al. examined the effect of varying tool plunge downforce on FSWed joints. They concluded that higher tool plunge downforce results in wider range of optimum conditions for friction stir welded joints. They also discovered that there are three types of defects depending on the FSW conditions: (i) large mass of flash (excess heat input); (ii) cavity or groove-like defects (insufficient heat input); and (iii) cavity due to abnormal stirring [28]. Leal and Loureiro studied the effect of varying tool feed on the formation of defect. They observed that defects were formed mainly on the advancing side of the weld. Also, the formation of voids increases with the increasing tool feed [35].

In real world scenario, fatigue strength of the joint is a greater problem as the material is rarely subjected to monotonic (either tensile or compressive) stress condition. The materials are subjected to cyclic stresses of varying stress ratios and hence the fatigue life of the material or the welds is more important [12,51]. Regarding the fatigue life of similar aluminium alloys, several studies have been performed and they reveal that the fatigue life of similar FSW joints at 10 million cycles is much lower than that of the base material [29, 44]. In case of dissimilar FSW, very limited research have been published regarding its fatigue life [11, 50]. Furthermore, the results revealed that fatigue life is also affected by the presence of defects in the weld. There is also an alloy dependence in the occurrence of these defects [34]. Various works [30] discuss the different reasons for the presence of these defects in FSW but no work has been published stating the optimum tool feed and rotational speed for the FSWed joints, without the inclusion of any defects.

In this study, the main objective is to find an optimum tool speed and feed which provides the maximum fatigue life for the butt FSW of AA5082 and AA7075 keeping the inclusions of welding defects at minimum. Micro-hardness and tensile property tests, and fractography has been performed on the AA5082-AA7075 butt FSW. As per the literature review, the study for the optimum condition for FSW of AA5082-AA7075 will be vital for industrial purposes.

3. Methodology

The Al alloys used for the study were 6 mm thick sheets of AA5082 and AA7075 which are in H19 and T651 conditions respectively. These materials were selected as there are similarities in the areas of their usages. Both AA5082 and AA7075 can be used for universal purposes. However, the main constraint for not being used universally is their cost of which AA7075 costs more. Accordingly, AA5082 finds its usage in the field of shipbuilding (marine), vehicle parts, automobile, and aerospace industries. AA5082 shows remarkable performance in severe environments such as under seawater and industrial chemical environment. It is prone to intergranular corrosion (IGC) and hence is not suitable for application in environments with high temperatures. AA7075 is not prone to IGC and hence can be used in high-temperature environments. However, its high cost restricts it from being used in the automobile industry and limits its application to aircraft and aerospace industries.

Dissimilar FSW butt joints of AA5082-AA7075 were produced under varying conditions and the impact of these varying welding conditions on the joint was investigated. The varying conditions for FSW are given in Table 1. The material of

Table 1
Varying conditions for the production of AA5082-AA7075 FSW butt joints

Sample No.	Speed (RPM)	Feed (mm/min)
1	900	25
2	900	40
3	900	63
4	1120	25
5	1120	40
6	1120	63
7	1400	25
8	1400	40
9	1400	63

the FSW tool used for the production of the test samples was HSS [31, 32]. The tool consists of three parts: shank, shoulder, and pin. The tool, as shown in Fig. 1 has a cylindrical shank and a shoulder of diameter 14.84 mm and 18.07 mm respectively. The pin was tapered with base diameter 5.9 mm and top diameter 3.15 mm. The vertical milling machine was used to produce the FSW butt welds. A fixture for holding the aluminium plates in place was designed and fabricated. Fig. 2 shows the setup prepared for the FSW. Tables 1 and Table 2 discuss various parameters used for preparing FSWed joints. More heat is generated in advancing side compared to retreating side. It is due to the fact that rotating tool swept the cooler material from advancing side to retreating side. Hence, for joining of dissimilar material low strength alloy is placed atadvancing side, so that more strength is generated at advancing side to increase the overall strength of welded joints. The contact surface on the plates was ground, to get rid of the oxide layer from the surface, using abrasive paper of grit size P600. The AA5082-AA7075 plates were butt welded using FSW. The welded plates were then machined to fabricate the test samples.

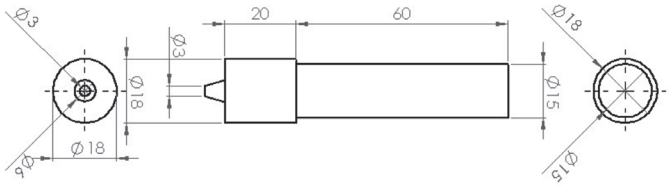

Fig. 1. Tool Design used for fabricating FSW Tool

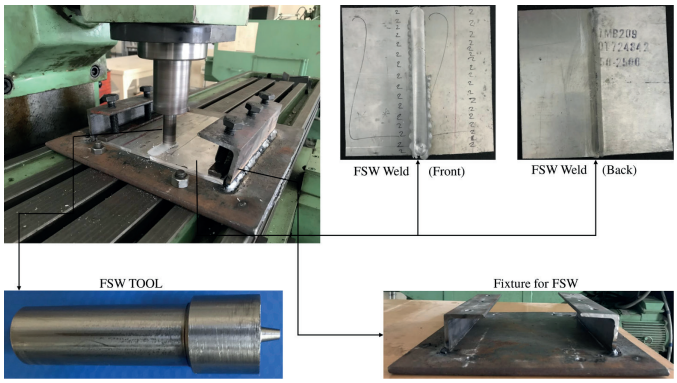

Fig. 2. Friction Stir Welding setup prepared for the HMT FN2V vertical milling machine

Table 2
Varying parameters of FSW

FSW Control	Parameters
Rotational Directions	Counter Clock Wise (CCW)
Advancing Side	AA5082
Retreating Side	AA7075

4. Experiment

The test samples for fatigue and tensile tests were prepared using ASTM E0466 [15] and ASTM E8M [16] standards respectively and the corresponding test samples are presented in Fig. 3. Fig. 4 shows an experimental flowchart for the tests performed on the samples. The monotonic stress (tensile) test was performed on a servo-hydraulic testing system with a load cell of 100 kN, at a strain rate of 5 mm/min. The resonance fatigue testing was performed and the stress ratio was set to $R = -1$,

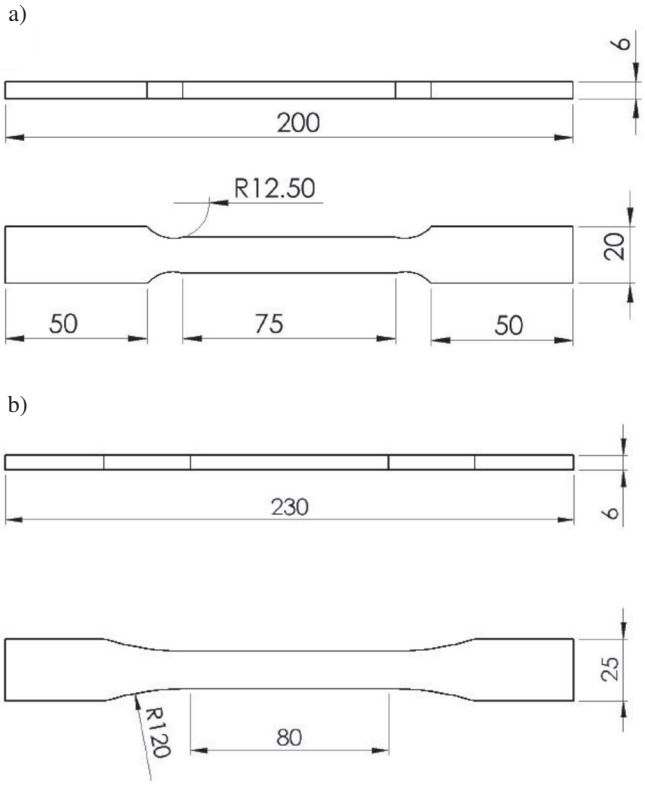

Fig. 3. a) ASTM E8M standard test specimen for tensile testing; b) ASTM E0466 standard test specimen for fatigue testing

fully reversed load condition. All the tests were performed at room temperature (23–27°C) with the relative humidity fluctuating from 15% to 20%. The rupture of the test sample was established as the stopping criterion for fatigue test. Fractography of the failed samples was performed using scanning electron microscope. For studying the micro-hardness, samples of size 30 mm × 2 mm × 6mm were machined and the tests were carried out on a Vickers hardness testing machine. A total of 56 indents were made starting from one base material to another with a gap of 0.5 mm and the load applied was 100 grams.

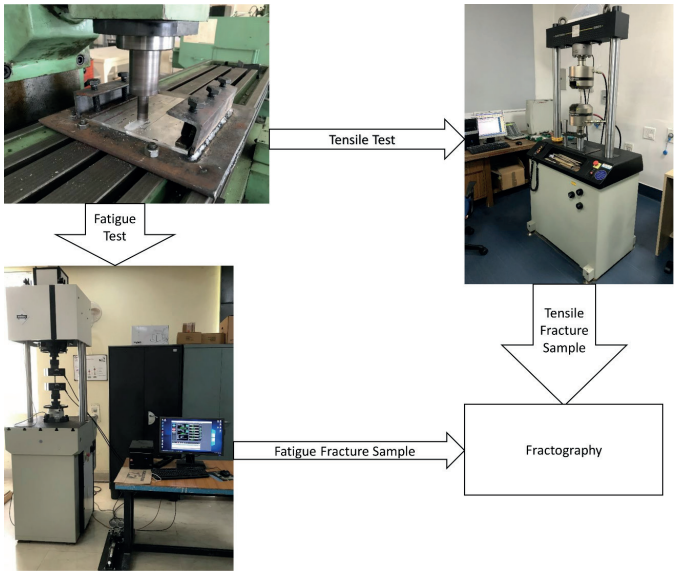

Fig. 4. Experimental sequence adopted for the tests to be performed

5. Result and discussions

5.1. ANOVA. Two-way ANOVA was performed on Minitab 19 and the results are presented in Table 3, 4, 5 and Fig. 5. Table 3 shows the factors that were considered for the analysis, namely tool rotational speed and tool feed. Table 4 presents the results obtained in the analysis. Here, DF is degree of freedom, SS is sum of squares, MM is mean of squares, F is the F-ratio and P is the P value. Table 5 provides the model summary where S represents how far the data values fall from the fitted values and is measured in the units of the response, R-Sq is the percentage of variation in the response that is explained by the model and is calculated as 1 minus the ratio of the error sum of squares to the total sum of squares and R-sq(adj) is the percentage of the variation in the response that is explained by the model, adjusted for the number of predictors in the model relative to the number of observations and is calculated as 1 minus the ratio of the mean square error to the mean square total. ANOVA was performed at 95% confidence, i.e. $\alpha = 0.05$. The three null hypotheses assumed for the two-way ANOVA are:

1. The tool rotational speed has no effect on the tensile strength of the weld.
2. The tool feed has no effect on the tensile strength of the weld.
3. The interaction of tool rotational speed and tool feed has no effect on the tensile strength of the weld.

As can be seen in Table 4, $P \leq \alpha$ for all the three cases, viz. tool rotational speed, tool feed and their interaction and hence all three null hypotheses are false. This shows that all these factors effect the tensile strength of the weld. Fig. 5 shows that the residual fall very close to the normal probability line. Accordingly, the variation of these process parameters was convincing to find the optimum conditions for production of FSWed AA5082-AA7075 butt joints.

Table 3
Factor Information

Factor	Type	Levels	Values
Tool Rotational Speed	Fixed	3	900, 1120, 1400
Tool Feed	Fixed	3	25, 40, 63

Table 4
Analysis of variance for UTM

Source	DF	SS	MM	F	P
Tool Rotational Speed	2	3723.2	1866.1	633.56	0.000
Tool Feed	2	24989.7	12494.9	4242.09	0.000
Tool Rotational Speed & Tool Feed Interaction	4	4494.9	1123.7	381.51	0.000
Error	18	53	2.9		
Total	26	33269.9			

Table 5
Model Summary

S	R-Sq	R-sq(adj)
1.71623	99.84%	99.77%

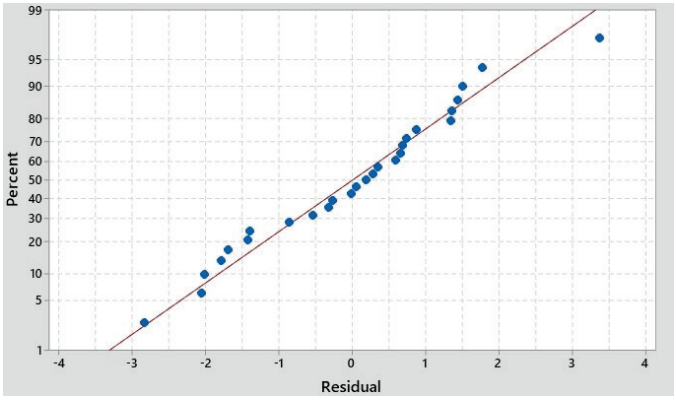

Fig. 5. Normal Probability Plot

5.2. Tensile test analysis. Table 6 and Fig. 6 present the tensile behaviour of the dissimilar FSW of AA5082-AA7075. The UTS for the welded joints was attained by the sample 5, that was welded at tool speed and feed 1120 rpm and 40 mm/min respectively, with an average UTS of 205.30 MPa. Fig. 7 and Fig. 8 shows the change in UTS corresponding to the change in tool speed and tool feed respectively. From Fig. 7 it is observed that as tool speed increases tensile strength increases up to a certain point. After that with increase in tool speed, strength decreases. It is due to the fact that after certain point that is 1120 rpm excess heat is generated. It creates turbulence in the heating zone. The same phenomena is observed with the variation of tool feed, as shown in Fig. 8. Heat generated due to slower tool speed is insufficient for the alloys to be welded properly which results in lower UTS. Also, at lower tool feed causes improper stirring of the material at the joint which decreases the UTS of the material [33]. The decrease in the UTS at higher tool speed is due to the high heat generation which causes surface defects to occur on the weld surface. The higher tool feed created turbulance in the weld zone which resulted in the introduction of pores in the weld zone. These surface and pores further decreases the strength of the weld. The joints failed AA5082 side which is in accordance with other studies on dissimilar FSW joints, where the failure occurred either at the TMAZ or the HAZ of the material with lower tensile strength [19, 44].

Table 6
Tensile Properties of FSW AA5082-AA7075 samples

Sample No.	Yield Strength (MPa) Offset 0.2%	Ultimate Tensile Strength (UTS) (MPa)	Young's Modulus (GPa)	Tensile extension at Yield Offset 0.2 % (mm)	Tensile strain at Maximum Load (%)
1	148.53	165.83	29.358	0.5165	1.65
2	149.46	190.27	29.571	0.5054	2.77
3	72.36	89.40	30.917	0.3127	0.35
4	141.88	157.59	26.422	0.5208	1.15
5	149.33	205.30	28.317	0.5213	3.10
6	138.60	142.64	29.432	0.4741	0.83
7	142.89	164.32	25.440	0.5332	1.22
8	138.90	155.52	27.290	0.5055	1.09
9	93.61	99.54	30.329	0.3793	0.45

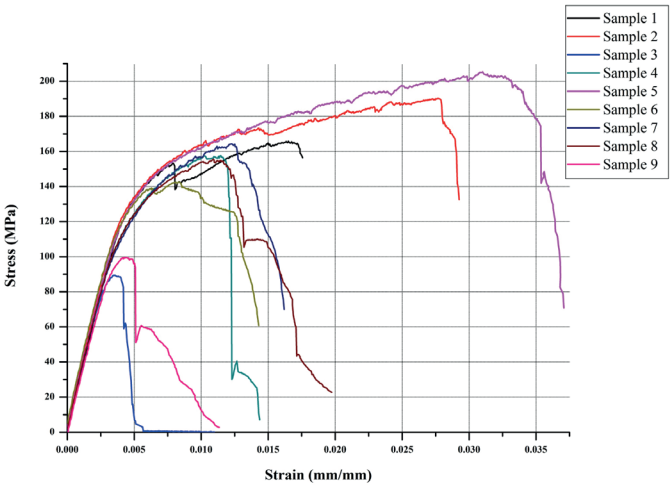

Fig. 6. Stress-Strain plot for FSW AA5082-AA7075 samples

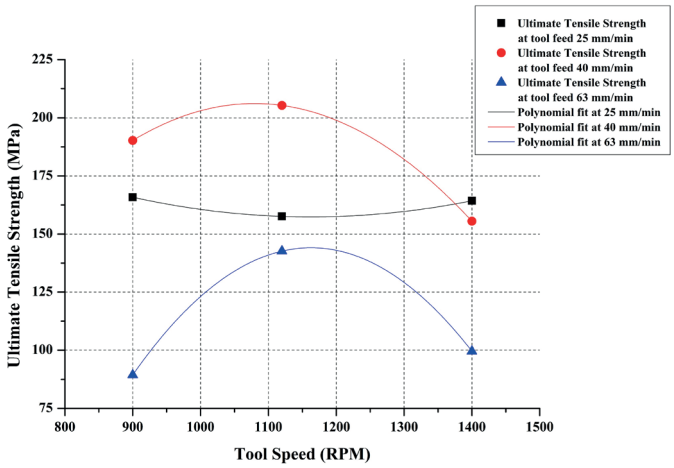

Fig. 7. Ultimate tensile strength vs. Tool speed comparison at different tool feed

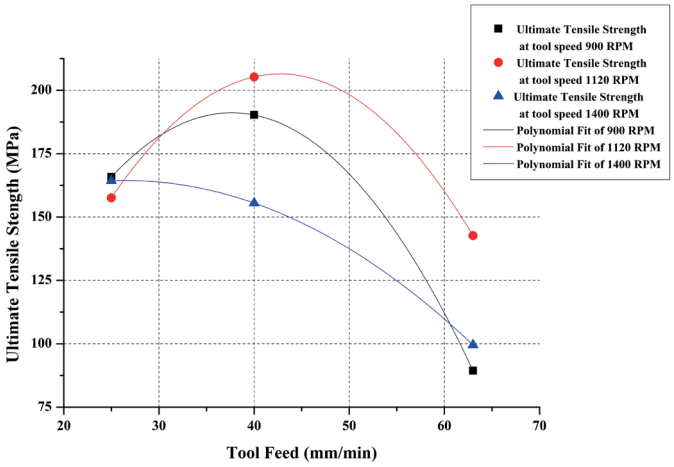

Fig. 8. Ultimate tensile strength vs. Tool feed comparison at different tool speed

5.3. Resonance fatigue analysis. Fatigue testings performed at the resonance frequency of the material being tested is termed as resonance fatigue analysis or tests. The RUMUL Testronic tests the material to find its resonance frequency and then performs the fatigue analysis at that frequency. It also modifies the frequency accordingly as the resonance frequency of the

material changes with the introduction of crack. The result of the resonance fatigue tests performed on the test samples at 40 MPa and 60 MPa stress amplitude is presented in Table 7 and Fig. 10. The results demonstrate that sample 2 (tool speed = 900 rpm and feed = 40 mm/min) has higher fatigue life at any given stress than the other samples tested. In other welded samples, defects were observed which were generated due to improper welding conditions. Surface defects and/or porosity, as shown in Fig. 9a and b, are observed in all the samples prepared except for sample 2. The presence of these welding defects is the reason for disagreement in the tensile test and fatigue failure test result. Also, these defects make it difficult to predict the fatigue life of the FSW joints. As can be seen from Table 7, the fatigue life for sample 4 and 7 at 60 MPa were quite different from the results of other samples. This is due to the presence of varying number and size of the defects present in the welds. In sample 2, no such defects were observed. For sample 2, fatigue test at different stress conditions were conducted and Fig. 11 shows its life in those stress conditions. In addition, S-N curve was also plotted on the basis of the fatigue test results. The S-N curve shows that the fatigue performance is quite significant in the lower range of applied stress.

Table 7
No. of cycles to failure at applied stress

Sample No.	No. of cycles to failure at 40 MPa	No. of cycles to failure at 60 MPa
1	86003	15001
2	2.27938E6	443870
3	84000	45002
4	108006	2005
5	479001	152000
6	158002	110000
7	155010	2000
8	19005	31000
9	79003	39002

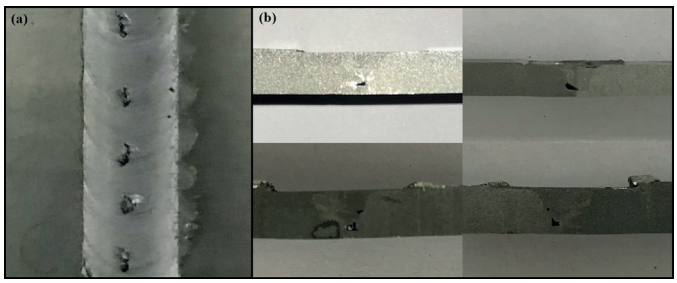

Fig. 9. a) Surface Defects which appear due to high tool rotational speed were observable in Samples 7, 8 and 9 due to high RPM; and b) Porosity which appear due to high tool feed were observable in Samples 3, 6 and 9. Sample 5 and 8 also displayed porosity at some points in the welded region

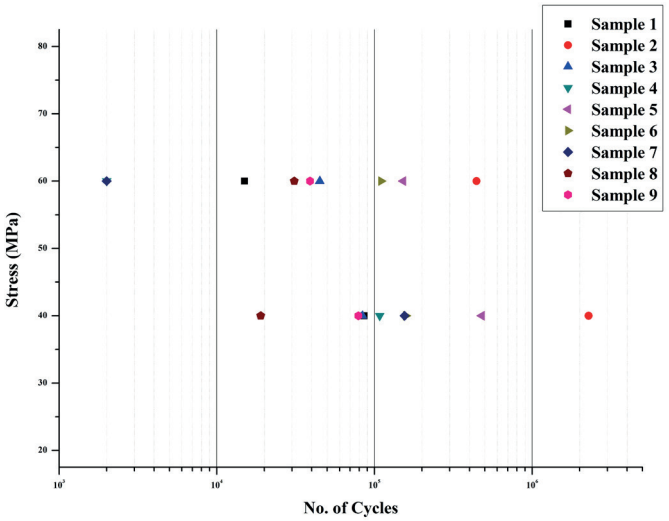

Fig. 10. Stress vs No. of cycles plot for all the FSW AA5082-AA7075 samples at 40 and 60 MPa (As the endurance strength, $\sigma_e = 0.4 \times UTS$, of all the samples varied between 35 MPA and 80 MPa, 40 MPa and 60 MPa were chosen for testing all the samples irrespective of their endurance strength)

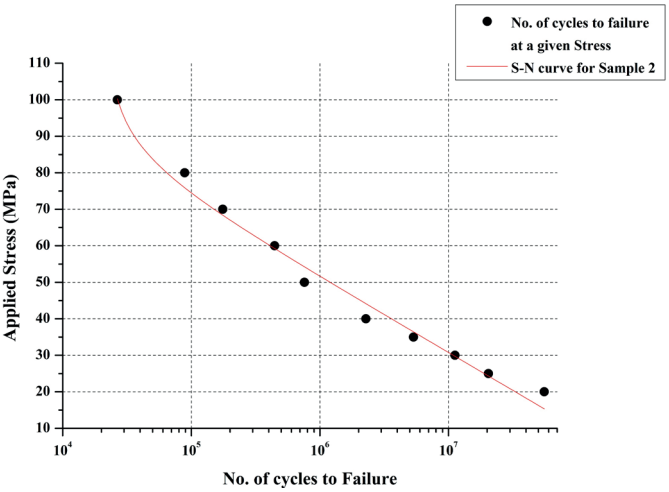

Fig. 11. Stress vs No. of cycles plot for Sample 2

Fig. 12 demonstrates a common trend of decrease in resonant frequency of the weld with an increase in the number of cycles. The rate of change of frequency depended on the UTS

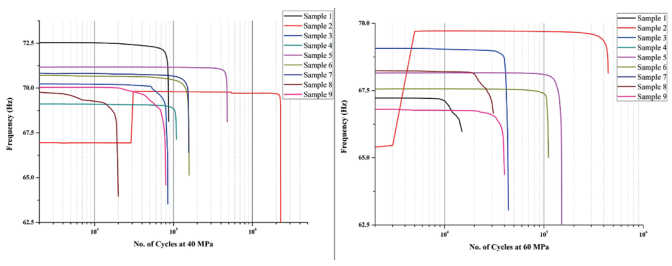

Fig. 12. Frequency vs No. of Cycles plot for FSW AA5082-AA7075 samples

and the size and number of defects present in the weld. Frequency change percentage, Fig. 13, can act as a reliable way of predicting the life of the welds in real time. It is observed that frequency change over 1% accounted to an exponential change in the frequency which always resulted in failure.

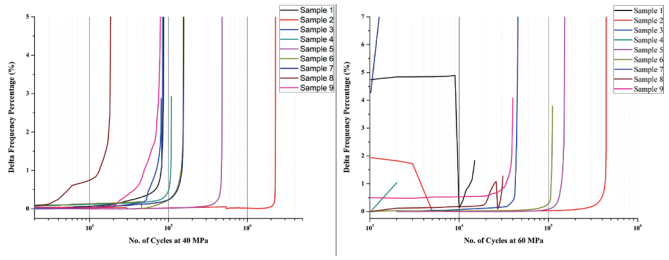

Fig. 13. Frequency Change Percentage vs No. of Cycles plot for FSW AA5082-AA7075 samples

5.4. Micro-hardness analysis. Fig. 14 demonstrates the microhardness test results for all the samples. These results exhibit a considerable change in the hardness of the weld zone in both the advancing and the retreating side. This change is due to the fact that different materials were used for welding. There is also a change in hardness of both the materials as the distance from the centre of the weld increases. The results illustrate that for every sample HAZ has the least hardness which lies around ± 7.5 mm to ± 1.25 mm from the centre of the weld. However, the hardness of the TMAZ, which lies around ± 2.5 mm to ± 7.5 mm from the centre of the weld, and the SZ, which lies from -2.5 mm to $+2.5$ mm, is considerably higher than the base material. The higher hardness in these zones is the result of dynamic recrystallization of the grains present in this region. Natural ageing of the material, at room temperature, may also be partly responsible for these variations in the hardness of the material. The hardness profile shows that there is a hardness minimum at the higher strength AA7075-T651 alloy side. This hardness loss is in the HAZ and is due to the overaged HAZ in the age-hardened AA7075-T651 [3, 22–25].

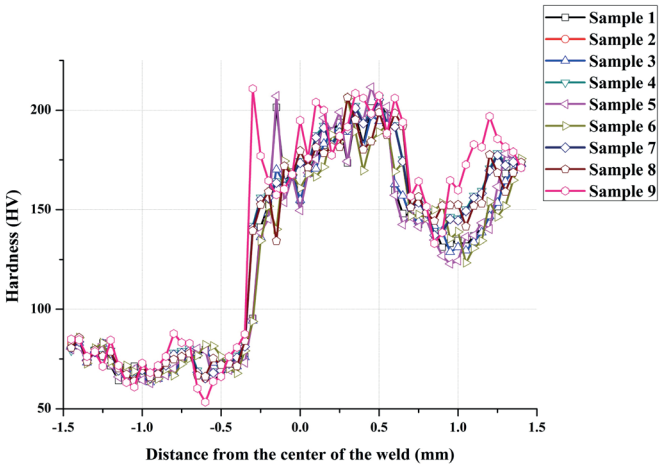

Fig. 14. Microhardness test result

5.5. Fracture analysis. Fig. 15 exhibits the fracture surface of FSW sample 2 that failed under fatigue loading. The growth of fatigue cracks is greatly confined to the normal stress plane and is thus does not depend upon properties of the material. At high stress intensity, crack growth is marked during each load cycle, this creates a band of markings along the fracture surface and these markings are referred to as striation. Striations help to determine the direction of crack growth. Striations start to disappear with decreasing stress intensities and only a weak band like pattern remains which helps to identify the direction of crack propagation [42, 45]. The centre of the striations was identified and the region around it is shown in Fig. 15a. Fig. 15b presents a magnified view of the region highlighted in Fig. 15a. In Fig. 15a and Fig. 15b, the area of growth of fatigue crack and the region of fast fracture is separated by the dotted line. The area on the left of the dotted line shows the presence of ridge like structures which depicts the area of fatigue crack growth. Whereas, the area on the right of the dotted lines show a flat plane area which depicts the region of fast fracture. The magnified view of the highlighted regions in Fig. 15b marked as A and B are shown in Fig. 15c and Fig. 15e, respectively. The magnified views of regions marked A1 and B1 Fig. 15c and Fig. 15e, respectively, are presented in Fig. 15d and Fig. 15f, respectively. The areas A, B, A1 and B1 shows the presence of striations which is evident due to the formation of ridge like structures

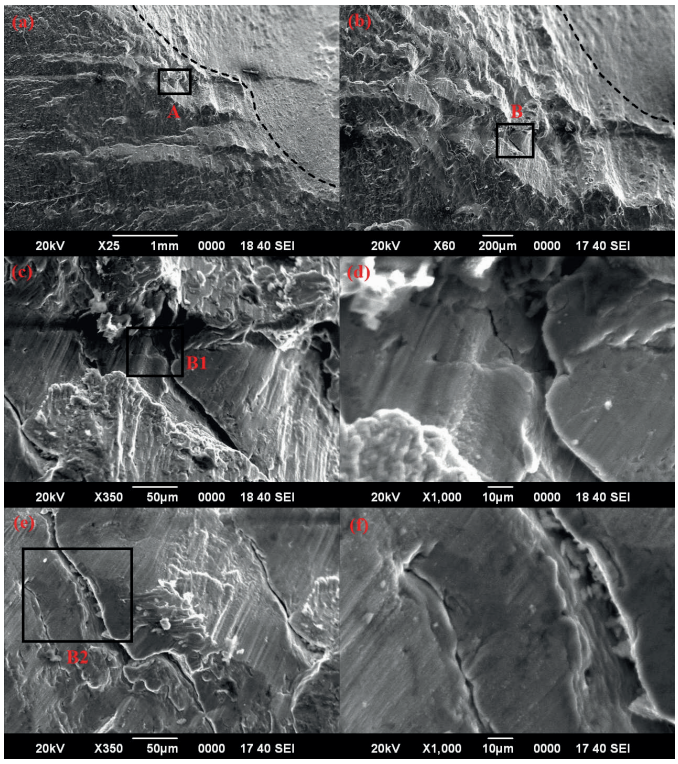

Fig. 15. a) Fracture surface of FSW sample that failed due to fatigue loading as seen under SEM; b) Magnified view of the highlighted region A, in the region of fatigue crack growth, showing ridge like formation; c) Magnified view of the region B showing striations and cracks; d) Magnified view of the region B1; e) Magnified view of the region B showing the possible crack initiation point; f) Magnified view of the region B2

during fatigue loading. These striations show that the fracture is ductile in nature for the region of fatigue crack growth [18]. In the region of fast fracture, the failure of the joint was immediate which exhibits the brittle nature of fracture in this region.

Fig. 16a exhibits the fracture surface of FSW sample 2 that failed under tensile loading. In ductile fracture, microvoids are formed during the material separation. These microvoids grow and ultimately fuse into larger voids during the plastic flow of materials. These larger voids are subjected to considerable amount of necking during the final phase of failure which contributes to the separation of these voids at the fracture surface. This phenomena causes the characteristic dimpled texture of a ductile fracture. If the separation is normal to the fracture plane, equiaxed or round dimples are formed. If the dimples are elongated, then shear stress is also involved in the fracture. The dimples are elongated in the direction of the shear [42,45]. Fig. 16b and Fig. 16c show the regions C and D, respectively, highlighted in Fig. 16a. Fig. 16d shows the magnified view of D2, highlighted in Fig. 16c and Fig. 16e shows the magnified view of D2, highlighted in Fig. 16d. Equiaxed dimples are observed in Fig. 16d and Fig. 16e. These equiaxed dimples demonstrate that the material failed under ductile fracture without the involvement of shear stresses.

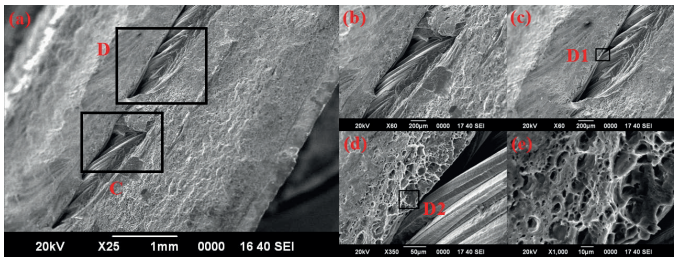

Fig. 16. a) Fracture surface of FSW sample that failed due to tensile loading as seen under SEM; b) Magnified view of the region C; c) Magnified view of the region D; d) Magnified view of the region D1 showing the presence of dimples; e) Magnified view of the region D2 showing that the dimples are equiaxed

Fatigue and tensile fracture surface analyses under SEM demonstrates the presence of striations and dimples, respectively, due to the ductile nature of the failure. For both fatigue and tensile samples, central and bottom zones of the welded surface were observed for the fracture morphology. However, no difference was observed in the fracture morphology of the central and the bottom zone which suggests a good penetration of the tool pin. Fatigue samples were characterized by the striations whereas the dimples characterised the tensile samples.

6. Conclusions

Fatigue and tensile behaviour of dissimilar butt FSW joints, with base materials AA5082 and AA7075, produced at varying tool speed and feed were studied. The following conclusions are presented:

- Ultimate tensile test of welded samples increases with increasing tool rotational speed and welding speed up to 1120 rpm and 40 mm/min respectively. From this point, further increase in tool rotational speed and welding speed decreases the strength of welded samples.
- Sample prepared at a tool rotational speed of 900 rpm and a tool travel speed of 40 mm/min, exhibited the best fatigue life as compared to other samples. This was due to the absence of defects such as pores and surface defects in this welded sample.
- FSW samples show the acceptable variation in SN curve. Fatigue life increases with decrease in stress applied. Below 40 MPa applied stress number of cycles required to fail the joint is of the order of 10^6 .
- It was observed that frequency change over 1% accounted to an exponential change in the frequency which always resulted in failure.
- The study of fracture surface for both fatigue and tensile tests demonstrates that fatigue and tensile fractures were ductile in nature. This was established by the presence of striations and dimples in fatigue and tensile fracture samples respectively.

From the above analysis it can be concluded that for fatigue life determination of FSW joints samples prepared at high ro-tational and travel speeds is good. In this study samples pre-pared at tool rotational speed 900 rpm and tool travel speed 40 mm/min shows best fatigue life. It is due to the fact that at high rotational speed adequate amount of heat generated, which softens the material properly. It leads to better stirring of mate-rial beneath the tool and produces a good quality FSW sample.

Acknowledgements. The authors would like to thank Dr. Prashant Prakash and Production Laboratory, BIT Mesra, Patna-Extn. for their help in the production of FSW Samples. In addition, the authors also acknowledges Department of Mechanical Engineering and Central Instrumentation Facility of Birla Institute of Technology, Mesra for its support in this research work.

References

[1] Y. Bozkurt, S. Salman and G. Çam, "Effect of welding parameters on lap shear tensile properties of dissimilar friction stir spot welded AA 5754-H22/2024-T3 joints", *Science and Technology of Welding and Joining* 18 (4), 337–345 (2013).

[2] G. Çam, "Friction stir welded structural materials: beyond Al-alloys", *International Materials Reviews* 56 (1), 1–48 (2011).

[3] G. Çam, S. Güçlüer, A. Çakan, and H. Serindag, "Mechanical properties of friction stir butt-welded Al-5086 H32 plate, Materialwissenschaft und Werkstofftechnik: Entwicklung, Fertigung, Prüfung", *Eigenschaften und Anwendungen technischer Werkstoffe* 40 (8), 638–642 (2009).

[4] G. Çam and G. İpekoğlu, "Recent developments in joining of aluminum alloys", *The International Journal of Advanced Manufacturing Technology* 91 (5-8), 1851–1866 (2017).

[5] G. Çam, G. İpekoğlu, T. Küçükömeroğlu, and S. Aktarer, "Applicability of friction stir welding to steels", *Journal of Achievements in Materials and Manufacturing Engineering* 80 (2), 65–85 (2017).

[6] G. Çam, G. İpekoğlu, and H. Tarık Serindağ, "Effects of use of higher strength interlayer and external cooling on properties of friction stir welded AA6061-T6 joints", *Science and Technology of Welding and Joining* 19 (8), 715–720 (2014).

[7] G. Çam and M. Koçak, "Microstructural and mechanical characterization of electron beam welded Al-alloy 7020", *Journal of Materials Science* 42 (17), 7154–7161 (2007).

[8] G. Çam and S. Mistikoglu, "Recent developments in friction stir welding of Al-alloys", *Journal of Materials Engineering and Performance* 23 (6), 1936–1953 (2014).

[9] G. Çam, V. Ventzke, J. Dos Santos, M. Koçak, G. Jennequin, and P. Gonthier-Maurin, "Characterisation of electron beam welded aluminium alloys", *Science and Technology of Welding and Joining* 4 (5), 317–323 (1999).

[10] G. Çam, V. Ventzke, J.F. Dos Santos, M. Koçak, M. Penasa, C. Rivela, and D. Boisselier, "Characterization of Laser and Electron Beam Welded Al Alloys, harakterisierung von laser-und elektronenstrahlgeschweißten Aluminiumlegierungen", *Prakt. Metallogr* 36 (2), 59–89 (1999).

[11] P. Cavaliere, A. De Santis, F. Panella, and A. Squillace, "Effect of welding parameters on mechanical and microstructural properties of dissimilar AA6082–AA2024 joints produced by friction stir welding", *Materials & Design* 30 (3), 609–616 (2009).

[12] L. Ceschini, I. Boromei, G. Minak, A. Morri, and F. Tarterini, "Effect of friction stir welding on microstructure, tensile and fatigue properties of the AA7005/10 vol.% Al_2O_3p composite", *Composites Science and Technology* 67 (3-4), 605–615 (2007).

[13] R. Crawford, G. Cook, A. Strauss, D. Hartman, and M. Stremler, "Experimental defect analysis and force prediction simulation of high weld pitch friction stir welding", *Science and Technology of Welding and Joining* 11 (6), 657–665 (2006).

[14] L. Dubourg, A. Merati, and M. Jahazi, "Process optimisation and mechanical properties of friction stir lap welds of 7075-T6 stringers on 2024-T3 skin", *Materials & Design* 31 (7), 3324–3330 (2010).

[15] A. E466-15, "Standard Practice for Conducting Force Controlled Constant Amplitude Axial Fatigue Tests of Metallic Materials", *ASTM International, West Conshohocken, PA* (2015).

[16] A. E. E8M-13, "Standard Test Methods for Tension Testing of Metallic Materials", *ASTM International, West Conshohocken, PA* (2013).

[17] M. Ericsson and R. Sandström, "Influence of welding speed on the fatigue of friction stir welds, and comparison with MIG and TIG", *International Journal of Fatigue* 25 (12), 1379–1387 (2003).

[18] A. Feng, D. Chen, and Z. Ma, "Microstructure and cyclic deformation behavior of a friction-stir-welded 7075 Al alloy", *Metallurgical and Materials Transactions A* 41 (4), 957–971 (2010).

[19] J. Guo, H. Chen, C. Sun, G. Bi, Z. Sun, and J. Wei, "Friction stir welding of dissimilar materials between AA6061 and AA7075 al alloys effects of process parameters", *Materials & Design* (1980–2015) 56, 185–192 (2014).

[20] V. Infante, D. Braga, F. Duarte, P. Moreira, M. De Freitas, and P. De Castro, "Study of the fatigue behaviour of dissimilar aluminium joints produced by friction stir welding", *International Journal of Fatigue* 82 (2), 310–316 (2016).

[21] G. İpekoğlu and G. Çam, "Effects of initial temper condition and postweld heat treatment on the properties of dissimilar friction-stir-welded joints between AA7075 and AA6061 aluminum alloys", *Metallurgical and Materials Transactions A* 45 (7), 3074–3087 (2014).

[22] G. İpekoğlu, S. Erim, and G. Çam, "Effects of temper condition and post weld heat treatment on the microstructure and mechanical properties of friction stir butt-welded AA7075 Al alloy plates", *The International Journal of Advanced Manufacturing Technology* 70 (1-4), 201–213 (2014).

[23] G. İpekoğlu, S. Erim, and G. Çam, "Investigation into the influence of post-weld heat treatment on the friction stir welded AA6061 Al-alloy plates with different temper conditions", *Metallurgical and Materials Transactions A* 45 (2), 864–877 (2014).

[24] G. İpekoğlu, S. Erim, B.G. Kıral, and G. Çam, "Investigation into the effect of temper condition on friction stir weldability of AA6061 Al-alloy plates", *Kovove Mater* 51 (3), 155–163 (2013).

[25] G. İpekoğlu, B.G. Kıral, S. Erim, and G. Çam, "Investigation of the effect of temper condition on friction stir weldability of AA7075 Al-alloy plates", *Material and Technology* 46 (6), 627–632 (2012).

[26] S. Jannet, P. Mathews, and R. Raja, "Comparative investigation of friction stir welding and fusion welding of 6061 T6 – 5083 O aluminum alloy based on mechanical properties and microstructure", *Bull. Pol. Ac.: Tech.* 62 (4), 791–795 (2014).

[27] N. Kashaev, V. Ventzke, and G. Çam, "Prospects of laser beam welding and friction stir welding processes for aluminium airframe structural applications", *Journal of Manufacturing Processes* 36, 571–600 (2018).

[28] Y. Kim, H. Fujii, T. Tsumura, T. Komazaki, and K. Nakata, "Three defect types in friction stir welding of aluminum die casting alloy", *Materials Science and Engineering: A* 415 (1-2), 250–254 (2006).

[29] İ. Küçükrendeci, "Mechanical and microstructural properties of EN AW-6060 aluminum alloy joints produced by friction stir welding", *Bull. Pol. Ac.: Tech.* 63 (2), 475–478 (2015).

[30] İ. Küçükrendeci, "The investigation of suitable welding parameters in polypropylene sheets joined with friction stir welding", *Bull. Pol. Ac.: Tech.* 67 (1), 133–140 (2019).

[31] G. Krolczyk, J. Krolczyk, R. Maruda, S. Legutko, and M. Tomaszewski, "Metrological changes in surface morphology of high-strength steels in manufacturing processes", *Measurement* 88, 176–185 (2016).

[32] G. Krolczyk, P. Nieslony, and S. Legutko, "Determination of tool life and research wear during duplex stainless steel turning", *Archives of Civil and Mechanical Engineering* 15 (2), 347–54 (2015).

[33] R. Kumar, B. Bora, S. Chattopadhyaya, G. Krolczyk, and S. Hloch, "Experimental and mathematical evaluation of thermal and tensile properties of friction stir welded joint", *International Journal of Materials and Product Technology* 57 (1-3), 204–229 (2018).

[34] R. Kumar, S. Chattopadhyaya, S. Hloch, G. Krolczyk, and S. Legutko, "Wear characteristics and defects analysis of friction stir welded joint of aluminium alloy 6061-T6", *Eksploatacja i niezawodność – Maintenance and Reliability* 18 (1), 128–135 (2016).

[35] R.M. Leal and A. Loureiro, "Defects formation in friction stir welding of aluminium alloys", In: *Materials Science Forum* 455, 299–302 (2004).

[36] C.Y. Lee, W.B. Lee, J.W. Kim, D.H. Choi, Y.M. Yeon, and S.B. Jung, "Lap joint properties of FSWed dissimilar formed 5052 Al and 6061 Al alloys with different thickness", *Journal of Materials Science* 43 (9), 3296–3304 (2008).

[37] W. Miller, L. Zhuang, J. Bottema, A. Wittebrood, P. De Smet, A. Haszler, and A. Vieregge, "Recent development in aluminium

alloys for the automotive industry", *Materials Science and Engineering: A* 280 (1), 37– 49 (2000).

[38] R.S. Mishra and Z.Y. Ma, "Friction stir welding and processing", *Materials Science and Engineering: R: Reports* 50 (1-2), 1–78 (2005).

[39] J. Mononen, M. Sirèn, and H. Hänninen, "Cost comparison of FSW and MIG welded aluminium panels", *Welding in the World* 47 (11-12), 32–35 (2003).

[40] R. Nandan, T. DebRoy, and H.K.D.H. Bhadeshia, "Recent advances in friction-stir welding–process, weldment structure and properties", *Progress in Materials Science* 53 (6), 980–1023 (2008).

[41] M. Pakdil, G. Çam, M. Koçak, and S. Erim, "Microstructural and mechanical characterization of laser beam welded AA6056 Al-alloy", *Materials Science and Engineering: A* 528 (24), 7350–7356 (2011).

[42] R.J. Parrington, "Fractography of metals and plastics", *Practical Failure Analysis* 2 (5), 16–19 (2002).

[43] H.M. Rao, J.B. Jordon, B. Ghaffari, X. Su, A.K. Khosrovaneh, M.E. Barkey, W. Yuan, and M. Guo, "Fatigue and fracture of friction stir linear welded dissimilar aluminum-to-magnesium alloys", *International Journal of Fatigue* 82 (3), 737–747 (2016).

[44] R.I. Rodriguez, J.B. Jordon, P.G. Allison, T. Rushing, and L. Garcia, "Low-cycle fatigue of dissimilar friction stir welded aluminum alloys", *Materials Science and Engineering: A* 654, 236–248 (2016).

[45] S.W. Song, B.C. Kim, T.J. Yoon, N.K. Kim, I.B. Kim, and C.Y. Kang, "Effect of welding parameters on weld formation and mechanical properties in dissimilar Al alloy joints by FSW", *Materials Transactions* 51 (7), 1319–1325 (2010).

[46] W. Thomas, "Friction stir joining of aluminium alloys", *TWI Bull* 6, 124–127 (1995).

[47] W. Thomas, "Friction stir process welds aluminium alloys", *Weld Journal* 41–45 (1996).

[48] W. Thomas, E. Nicholas, J. Needham, M. Murch, P. Temple-Smith, and C. Dawes, "Friction Stir Butt Welding, International Patent Appl. n. PCT/GB92/02203 and GB Patent Appl. n. 9125978.8. US Patent, (5,460,317)", (1991).

[49] W. Thomas, P. Threadgill, and E. Nicholas, "Feasibility of friction stir welding steel", *Science and Technology of Welding and Joining* 4 (6), 365–372 (1999).

[50] Y. Uematsu, Y. Tozaki, K. Tokaji, and M. Nakamura, "Fatigue behavior of dissimilar friction stir welds between cast and wrought aluminum alloys", *Strength of Materials* 40 (1), 138–141 (2008).

[51] W. Więckowski, P. Lacki, and J. Adamus, "Examinations of steel overlap joints obtained using the friction stir welding technology", *Arch. Metall. Mater.* 64 (1), 393–399 (2019).